Recent advances of the Ti:sapphire-pumped high-repetition-rate femtosecond optical parametric oscillator

P. E. Powers, R. J. Ellingson, and W. S. Pelouch

School of Applied and Engineering Physics, Cornell University, Ithaca, New York 14853

C. L. Tang

School of Electrical Engineering, Cornell University, Ithaca, New York 14853

Received December 17, 1992

The details concerning the resonator configuration, crystal parameters, and operating characteristics of high-repetition-rate and high-average-power broadly tunable femtosecond optical parametric oscillators are reviewed and discussed in some detail. We also report new results on an intracavity-doubled optical parametric oscillator with tunability from 580 to 657 nm in the visible and the first, to our knowledge, high-repetition-rate femtosecond optical parametric oscillator with the new nonlinear-optical crystal In:$KTiOAsO_4$, which can potentially tune to 5.3 μm.

INTRODUCTION

One of the most active new directions of research on optical parametric oscillators[1] (OPO's) is on broadly tunable high-repetition-rate femtosecond OPO's. To generate a peak power large enough to overcome the OPO's threshold, the first high-repetition-rate OPO was coupled intracavity to a colliding-pulse mode-locked dye laser.[2-4] This OPO generated 100-fs pulses at 80 MHz with ~3 mW of average power. After this initial development came a rapid improvement in design simplicity and performance. The first externally pumped high-repetition-rate femtosecond OPO with a high-power hybridly mode-locked dye laser permitted considerable design simplification.[5] This was quickly followed by a demonstration in which the OPO was externally pumped with a high-power high-repetition-rate femtosecond Ti:sapphire laser.[6,7] With the external-cavity Ti:sapphire-pumped OPO the design is simple and the performance robust. The Ti:sapphire-pumped OPO has generated hundreds of milliwatts in both the signal branch (to as much as 680 mW) and the idler branch (to more than 450 mW), adding to more than 1 W of frequency-converted power. The femtosecond Ti:sapphire-pumped OPO has also demonstrated extensive tunability,[8] making it an extremely attractive device for femtosecond applications. In this paper we present a detailed description of the design parameters and the operating characteristics of a Ti:sapphire-pumped femtosecond OPO as well as the most recent results of our use of this device.

FEMTOSECOND OPTICAL PARAMETRIC OSCILLATOR CAVITY DESIGN CONSIDERATIONS

Included in the considerations for designing a femtosecond Ti:sapphire-pumped OPO are the configuration of the resonator and the orientation of the nonlinear crystal. The basic OPO cavity is simple. It can be configured as either a linear or a ring cavity, with or without intracavity dispersion compensation. Since the device is synchronously pumped the cavity length must match that of the Ti:sapphire laser. These geometries are shown in Fig. 1. Both cavities are singly resonant with single-stack mirrors reflecting either the signal or the idler wave. Besides the geometrical differences between these two configurations, the main feature that sets them apart is that as the resonated wave traverses one round trip the pulse passes through the nonlinear crystal twice in the linear cavity and only once in the ring cavity. The advantage of the linear cavity is that it permits double passing of the pump in the nonlinear crystal. This has led to as much as a 20% increase in power in the output of the signal beam.[7] When single-pass pumping fails to bring the OPO comfortably above threshold double passing the pump may permit the OPO to operate well above threshold, resulting in better stability and power. However, the two passes of the signal beam through the crystal lead to more dispersion of the pulse, of which only the linear group-velocity dispersion (GVD) can be compensated for by the prism sequence. The losses from the extra pass through the crystal are more than compensated for by backreflecting the pump. The linear cavity with a backreflected pump does require that the Ti:sapphire pump laser be either feedback insensitive or optically isolated from the backreflection. We used a Ti:sapphire laser that was configured in a ring for double passing the pump because this configuration was not feedback sensitive.[9] The ring-cavity OPO eliminates the second pass through the crystal but does not permit double passing of the pump. When pumped high enough above threshold, the ring-cavity-OPO operation is as robust as the linear cavity with feedback.

0740-3224/93/112162-06$06.00

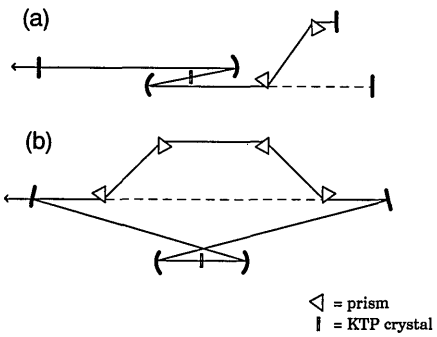

Fig. 1. Schematic of (a) a linear and (b) a ring OPO cavity with (solid lines) or without (dashed lines) intracavity-prism dispersion compensation. The Ti:sapphire pump laser is not shown because its alignment to the crystal depends on whether a type-I or a type-II interaction is chosen and whether the *e* wave or the *o* wave is resonated. Note that for a round trip the pulse passes through the crystal twice for the linear cavity and only once for the ring cavity.

The alignment of the Ti:sapphire pump with the OPO cavity depends on whether the *o* wave (idler) or *e* wave (signal) is resonated. When the idler is resonated the pump and idler should be collinear to maximize the gain. Resonating the signal, however, requires determining how the Poynting vector of the signal walks off the pump. Wachman *et al.*[8] first noticed that the OPO oscillated such that the Poynting vector of the pump and signal were collinear. Hence the pump must be offset from the signal to permit the Poynting vector of the signal to walk onto the pump. This is accomplished by use of a noncollinear phase-matching geometry such that the noncollinear angle between the pump and the signal is equal to the negative of the walk-off angle. The Poynting vector of the signal then walks onto the pump wave and not away from it. The crystal orientation is shown in Fig. 2. Figure 3 plots the value of the Poynting-vector walk-off as a function of the phase-matching angle. In the case of large phase-matching angles this walk-off is small, permitting alignment of the pump through one of the OPO-cavity mirrors. For smaller phase-matching angles the walk-off angle increases, and the pump and OPO-cavity mirrors must be positioned to permit this walk-off. For example, the noncollinear angle for KTP with a type-II interaction is 2.9° at a phase-matching angle of 45°. Using cavity mirrors of $R = 10$ cm curvature would then require that the pump and signal beams be ~4 mm apart at a distance of 5 cm from the KTP crystal.

Suitable focusing parameters for the OPO cavity and the Ti:sapphire pump are determined by considering the respective focused beam sizes inside the crystal and the angular acceptance of the crystal. The theoretical calculations of Cheung and Liu[10] show that, for a configuration in which the Poynting vectors of the pump and resonated wave are collinear, their focused beam sizes in the crystal should be approximately the same. The number of possible focusing combinations that result in equal beam sizes of the pump and signal in the crystal is limited by the fact that not all these focusings will permit oscillation. As the beam waist increases, the peak intensity decreases eventually to a point below the OPO threshold. At the other extreme, when the focused beam size decreases, the angular spread of the focused beam becomes larger than the acceptance angle of the crystal, which then reduces the efficiency of the phase-matched interaction. The angular acceptance can be calculated by plotting the function

$$\left[\frac{\sin(\Delta k l_c/2)}{\Delta k l_c/2}\right], \qquad \Delta\mathbf{k} = \mathbf{k}_p - \mathbf{k}_s - \mathbf{k}_i \tag{1}$$

as a function of the phase-matching angle, where Δk is the phase mismatch and l_c is the crystal length. The full width at half-maximum (FWHM) gives the angular acceptance. For a 1-mm-thick crystal the angular-acceptance angle for KTP in the x–z plane is 0.75° for a pump wavelength of 780 nm and a signal wavelength of 1.3 μm. If the OPO's beam diameter is 1 mm, then the focus that matches the crystal's angular acceptance is 7.6 cm (R = 15.2 cm).

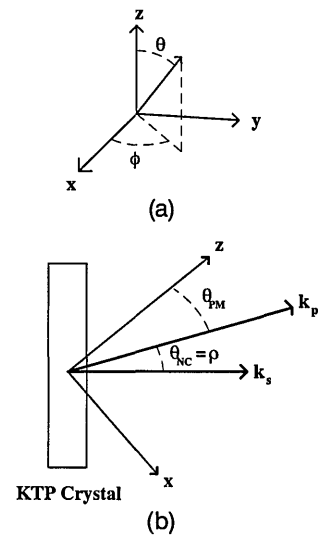

Fig. 2. Crystal orientation. (a) The angles θ and ϕ are defined. (b) The alignment of the KTP crystal for a type-II interaction in which the *e* wave ($\mathbf{k}_s$) is resonated. The pump ($\mathbf{k}_p$) and $\mathbf{k}_s$ lie in the x–z plane at a noncollinear angle that is equal to the negative of the walk-off angle ρ. $\mathbf{k}_s$ is oriented so that its Poynting vector walks onto the pump.

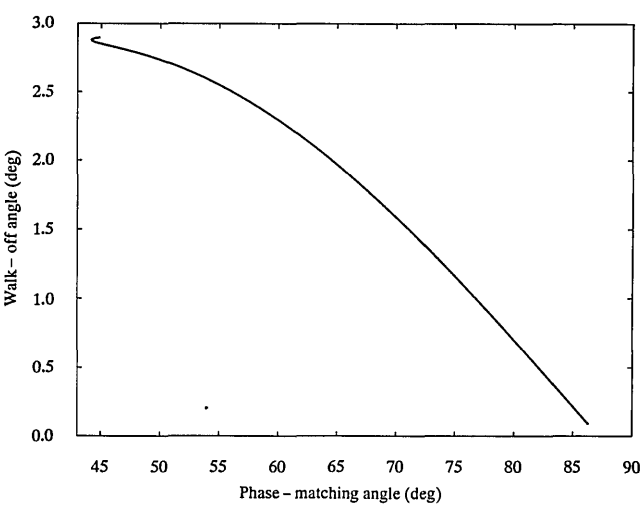

Fig. 3. The Poynting-vector walk-off of the signal from the pump is plotted as a function of the phase-matching angle for a 780-nm pump and a noncollinear angle of 2.8°.

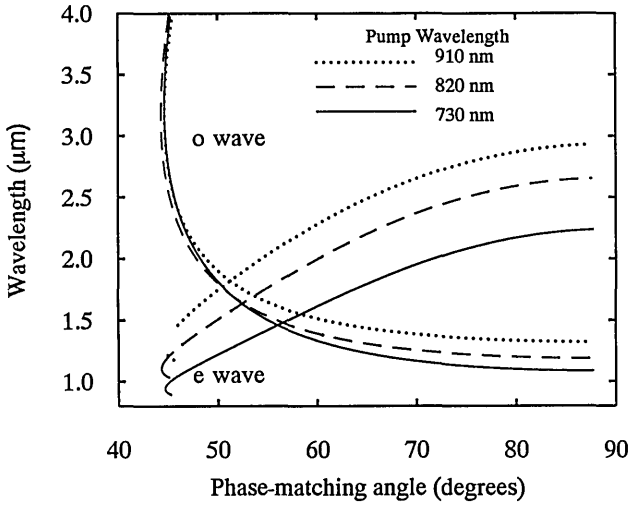

Fig. 4. Tuning curves for a type-II interaction in KTP with a noncollinear angle of 2.8°. The tuning curves for three pump wavelengths covering a large part of the Ti:sapphire's tuning range illustrate the effect of tuning the pump.

In an attempt to optimize the focusing, we varied the cavity focusing mirrors from $R = 7.5$ cm to $R = 20$ cm; corresponding to these changes we varied the pump focus from $R = 10$ cm to $R = 30$ cm so as to keep the signal- to pump-beam-waist ratio approximately constant. We found that with mirrors with a higher radius of curvature the OPO operated nearer to threshold and that at too tight a focus the OPO would not oscillate at all (at $R = 7.5$ cm). Our best performance has been with either $R = 10$ cm or $R = 15$ cm for the OPO-cavity mirrors and either $R = 15$ cm or $R = 25$ cm, respectively, for the pump focusing mirror.

CRYSTAL ORIENTATION

Critical to the successful operation of a femtosecond OPO is the orientation of the nonlinear crystal. In this section we use the properties of the nonlinear crystal KTP as an example to clarify how to determine the alignment that maximizes the gain. The first consideration is to orient the crystal such that the effective second-order nonlinearity, d_{eff}, is maximized. For KTP, d_{eff} is approximated by[11,12]

$$\text{Type I} \quad d_{\text{eff}} = 1/2(d_{15} - d_{24})\sin(2\theta)\cos(2\phi), \tag{2}$$

$$\text{Type II} \quad d_{\text{eff}} = -[d_{15}\sin^2(\phi) + d_{24}\cos^2(\phi)]\sin(\theta), \tag{3}$$

where θ, the phase-matching angle, and ϕ are defined as in Fig. 2 above. For KTP the values of d_{15} and d_{24} are 2.04 and 3.92, respectively.[13] For these values the type-II interaction always has a larger d_{eff} than does the type-I interaction. For the type-II interaction d_{eff} is maximized for $\phi = 0$ so that the KTP crystal is aligned such that the parametric interactions occur in the x–z plane. It is clear from Eq. (3) that one maximizes d_{eff} for the type-II interaction for a phase-matching angle of 90°; however, it is sometimes advantageous to phase match at smaller angles. Specifically, wavelengths that are not available at larger angles are accessible at smaller phase-matching angles, as shown in Fig. 4.

The tuning curves for KTP with $\phi = 0$ and for various possible Ti:sapphire pump wavelengths are generated as a function of the phase-matching angle θ and are shown in Fig. 4. From this figure it is clear that KTP has a broad tuning range, but to have access to the whole range requires either tuning the pump or changing the crystal phase-matching angle. The Ti:sapphire-pumped OPO offers the advantage that the Ti:sapphire laser itself is tunable, which leads to broad tunability in the OPO. As seen in Fig. 4, tuning the Ti:sapphire laser can lead to a substantial change in wavelength in the OPO. For the region in which θ is $<55°$, tuning the pump leads to a large change in the e wave's wavelength but only a small change in the o wave. In this region one accomplishes tuning to the longer wavelengths of the o wave by simply changing the phase-matching angle. For angles that are $>55°$, in which d_{eff} is largest, changing the phase-matching angle leads to a small change in wavelength, so in this region tuning the pump makes more sense.

A consideration that has a direct bearing on the performance of the OPO is the magnitude of the inverse group-velocity mismatch (GVM) between the pump, the signal, and the idler waves. The GVM is approximately -25 fs/mm between the pump and the signal and ~ 200 fs/mm between the pump and the idler for the majority of the tuning range. This puts a limitation on the crystal's thickness. The crystal should be thick enough to provide high gain but thin enough to limit the effect of GVM.

Additionally, the crystal should be thin enough to phase match the bandwidth of the ultrashort pulse. We generated pulses as short as 57 fs by using a 1.15-mm-thick crystal, with 115 mW in the signal beam. With this 1.15-mm-thick crystal we measured up to 60% pump depletion. Although using a thicker crystal will increase the interaction length and will lead to more power, this has the potential of broadening the OPO pulses. The FWHM of Eq. (1) plotted versus wavelength gives the phase-matching bandwidth. The phase-matching bandwidth for a 1-mm-thick crystal of KTP is 33 nm at a signal wavelength of 1.3 μm; this has a transform-limited pulse width of 53 fs, assuming a sech^2 pulse shape. Increasing the crystal thickness to 1.5 mm decreases the phase-matching bandwidth to 22 nm, and consequently the transform-limited pulse width is 80 fs.

OPERATING CHARACTERISTICS

When the OPO is pumped sufficiently above threshold (1 W at 100 fs or better), the output of the OPO is a stable pulse train. The average-power fluctuations and pulse-to-pulse variations of the OPO are determined almost entirely by the Ti:sapphire pump laser. Even without an active cavity-length stabilizer to length match the OPO and Ti:sapphire cavities continuously, oscillation can be maintained stably for as much as several hours. Operating near threshold decreases the stability of the OPO pulse train, as does operating near 0 GVD.

The OPO pulses are characterized by a chirped and an unchirped regime. The chirped regime is encountered when the cavity is operated with a net positive GVD, and the unchirped regime occurs with net negative GVD. With intracavity dispersion compensation it is possible to vary the GVD from net negative values to net positive values. We observed a flip from chirped pulses to unchirped pulses as we changed from negative to positive net GVD.

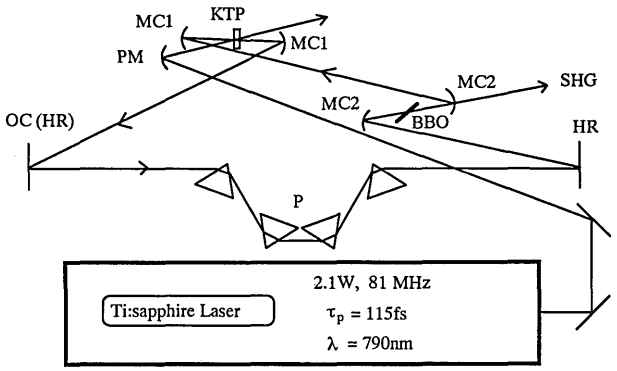

Fig. 5. Ti:sapphire-pumped intracavity-doubled KTP OPO. The Ti:sapphire beam is focused by the $R = 25$ cm pump mirror (PM) onto the 1.5-mm-thick KTP crystal. The KTP gain crystal is cut at $\theta = 45°$, $\phi = 0°$ for type-II phase matching in the positive region of the x–z plane. The OPO curved mirrors (MC1, MC2) at the gain and frequency doubling foci have radii $R = 15$ cm and $R = 10$ cm, respectively. Two pairs of SF-14 prisms (P) spaced 20 cm tip to tip are used for intracavity dispersion compensation. The single SHG output is transmitted through the OPO high reflector (HR) at the doubling focus. OC, output coupler; τ_p, pulse width.

Near the 0 GVD point the pulses spontaneously jump between chirped and unchirped pulses, leading to instability in the pulse train.

Accompanying the signal and idler outputs are several non-phase-matched processes. Non-phase-matched second-harmonic generation (SHG) of the signal wave ($e + e \rightarrow e$), as well as noncollinear non-phase-matched sum-frequency generation between the pump and the signal wave ($o + e \rightarrow o$), have been identified.[6,7,14] We have also identified the noncollinear non-phase-matched sum-frequency generation between the pump and the idler wave. The power in this beam is less than a milliwatt. It is interesting that this wavelength is equal to the non-phase-matched second harmonic (SH) of the signal beam when the signal beam equals 1.5 times the pump beam. We have observed this with a 867-nm pump and 1.3-μm signal. With the signal and idler pulses this gives five synchronous wavelengths.

RECENT ADVANCES

Our most recent efforts have been directed toward generating exceptionally high output powers and broad tunability. For the high-power result we used a Ti:sapphire laser, producing 2.4 W of average power with a 115-fs pulse width. With this pump source we generated 130-fs, 680-mW pulses in the signal branch by using a linear-cavity OPO configuration and a 1.5-mm-thick KTP crystal. This is excellent conversion efficiency and is near the Manley–Rowe limit. The Manley–Rowe relation states that the number of pump photons that are annihilated is equal to the number of signal–idler photon pairs that are created.[15] The limit for a 2.4-W pump at 780 nm and a signal wavelength of 1.3 μm yields 720 mW in the signal beam.

Using intracavity frequency doubling, we have extended into the visible the wavelength range that is accessible to femtosecond OPO pulses. Because the Ti:sapphire-pumped OPO is synchronously pumped, the nonlinear loss of the SHG to the intracavity OPO-signal pulse does not destroy the pulse-shaping process. We generated a total of 240 mW of sub-100-fs pulses at a wavelength of 647 nm and demonstrated tuning of the output from 580 to 657 nm. Because of the optical-power limiting by the nonlinear loss of the SHG,[14] the output of the intracavity-doubled OPO is very stable and quiet. Although no quantitative noise measurements have been made, the output pulse train of the SH is as quiet as the Ti:sapphire laser when viewed on a fast oscilloscope.

The intracavity-doubled OPO, which uses a 1.5-mm-thick KTP crystal that is cut for type-II ($o \rightarrow e + o$) phase matching ($\theta = 45°$, $\phi = 0°$) in the x–z plane, is shown in Fig. 5. We add to the ring cavity an additional intracavity focus of $R = 10$ cm mirrors that are high reflectors centered at 1.3 μm and that transmit ~80% of the SH wavelength. After aligning the OPO with the additional intracavity focus, we use the OPO-signal beam, taken through a 1% output coupler, to align the 47-μm-thick β-BaB_2O_4 (BBO) Brewster-cut crystal for SHG using type-I phase matching. Next we insert the thin BBO crystal at the intracavity focus, regain OPO oscillation, and proceed to replace the OPO's 1% output coupler with a high reflector to maximize the SH output power.

BBO is exceptionally well suited for frequency doubling of ultrashort pulses in the wavelength range of the signal branch of the OPO. The phase-matching curve for SHG in BBO is shown in Fig. 6(a). We refer to the point on the

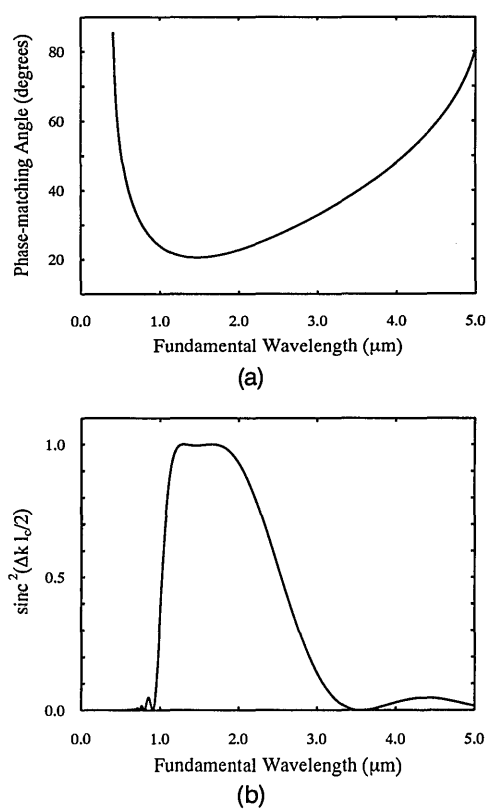

Fig. 6. (a) Phase-matching angle versus fundamental wavelength for type-I SHG in BBO. The degenerate point at which the phase-matching angle is minimized and phase matches a single wavelength occurs at 1.47 μm. The SHG phase-matching bandwidth becomes very large near this degenerate point. (b) The SHG phase-matching spectrum for $l_c = 55$ μm BBO crystal (47-μm-thick crystal at Brewster's angle) that was phase matched for SHG at 1.3 and 1.65 μm.

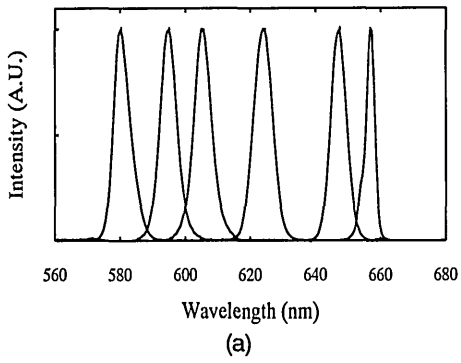

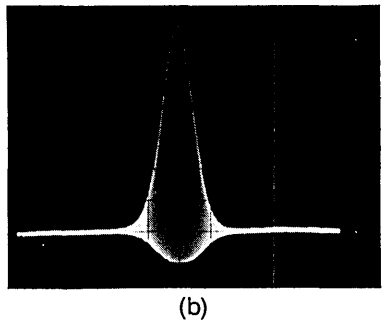

Fig. 7. (a) Intracavity-doubled KTP OPO spectra within the demonstrated tuning range of 580–657 nm. (b) Real-time interferometric autocorrelation for 240-mW total SH produced, at 115-fs pulse width, centered at 647 nm. Although not shown, extracavity two-prism dispersion compensation compressed the pulses to 95 fs with no degradation in pulse shape.

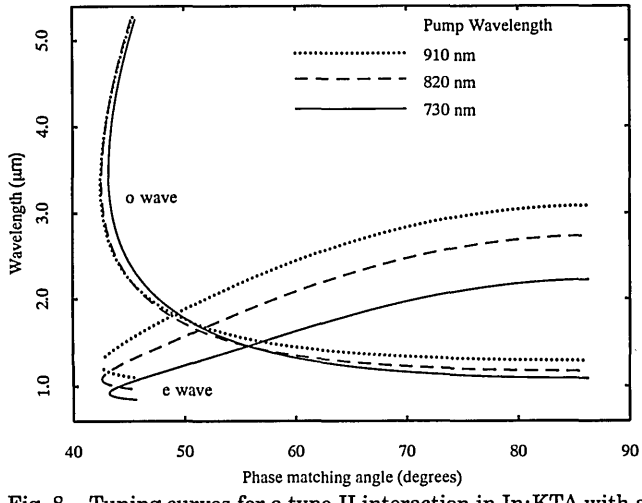

Fig. 8. Tuning curves for a type-II interaction in In:KTA with a noncollinear angle of $-2.8°$. The tuning curves for three pump wavelengths covering a large part of the Ti:sapphire's tuning range illustrate the effect of tuning the pump.

phase-matching curve at which the slope is zero as the degenerate point. Interestingly, at this degenerate point in the phase-matching curve, which occurs for BBO at ~1.47 μm, the group velocities of the fundamental and SH are matched. As a result, in the regime of 1.47-μm BBO has a small GVM and a large SHG phase-matching bandwidth. It is important to note that this simultaneous matching of the SHG phase and group velocities at the degenerate point also occurs in $LiNbO_3$, another crystal of the $3m$ point group.

In the case of our ultrathin 47-μm-thick BBO crystal the phase-matching bandwidth for 1.3 μm is shown in Fig. 6(b). The two $\text{sinc}^2(\Delta k l_c/2)$ SHG phase-matching curves (at $\lambda = 1.30$ μm and $\lambda = 1.65$ μm) have merged to give a FWHM SHG bandwidth of 1514 nm. Our observations of the intracavity-doubled OPO agree: after tuning the OPO from 1.2 to 1.3 μm, rotating the phase-matching angle of the BBO has no effect on the SHG conversion efficiency. Once the BBO crystal is aligned to double near the center of the OPO-signal tuning curve, tuning the SHG is accomplished by simply tuning the OPO with no adjustment to the BBO phase-matching angle.

As mentioned above, the intracavity-doubled OPO is a stable source of femtosecond pulses in the visible. Figure 7 shows spectra from the demonstrated tuning range and a real-time interferometric autocorrelation of the SHG output. The pulse shape of the OPO fundamental is similarly clean and quiet. The Ti:sapphire-pumped femtosecond OPO and the intracavity-doubled OPO demonstrate very powerful nonlinear-optical-generation techniques that will continue to increase in importance as pump sources are improved and as new pump sources are developed.

To extend the tuning range to longer wavelengths, beyond 4 μm, we have demonstrated optical parametric oscillation with the new nonlinear crystal In:$KTiOAsO_4$ (In:KTA). In:KTA is very similar to KTP but has a larger transparency range, which extends to 5.3 μm. In:KTA's transparency range has no absorption bands as does KTP, for example, at 3.5 μm.[16] Figure 8 shows that phase matching over the transparency region for In:KTA is possible out to 5.3 μm. The In:KTA OPO is aligned in the same way as the KTP OPO.[7] A 1.5-mm-thick In:KTA crystal is oriented for a type-II interaction with a phase-matching angle of ~50°. The e wave is resonated in a linear cavity with prisms with a noncollinear angle that is equal to the negative of the walk-off angle of 2°. We produced pulses at 1.435 μm in the signal branch and 1.662 μm in the idler branch with a 770-nm Ti:sapphire pump. This is the first demonstration, to our knowledge, of a high-repetition-rate OPO with In:KTA, and, as shown in Fig. 8, tuning beyond 4 μm is possible with the appropriate crystal cut and mirror coatings.

CONCLUSION

The high-repetition-rate Ti:sapphire-pumped femtosecond OPO is a robust device that is capable of high average power and short pulse widths, tunable from the visible to the mid-IR. This device produced unchirped pulses with powers as high as 680 mW, pulse widths as short as 57 fs, and tunability from 580 to 657 nm in the visible as well as from 1.16 to 2.2 μm in the IR. In the near future we plan to extend this tuning range to 5 μm with In:KTA, and we are looking at other new materials that would permit us to tune even further into the IR. At the same time, we are also looking into generating OPO pulses that are shorter than 57 fs, to our knowledge the shortest pulses from an OPO yet reported. Finally, as a true test of the OPO's performance, we plan to use the OPO in pump–probe-style experiments to generate high signal-to-noise data.

ACKNOWLEDGMENTS

This research was supported by the Joint Services Electronics Program and the National Science Foundation.

REFERENCES AND NOTES

1. See, e.g., C. L. Tang, W. R. Bosenburg, T. Ukachi, R. J. Lane, and K. L. Cheng, Proc. IEEE **80,** 365 (1992), and the references therein.
2. D. C. Edelstein, E. S. Wachman, and C. L. Tang, Appl. Phys. Lett. **54,** 1728 (1989).
3. E. S. Wachman, D. C. Edelstein, and C. L. Tang, Opt. Lett. **15,** 136 (1990).
4. E. S. Wachman, W. S. Pelouch, and C. L. Tang, J. Appl. Phys. **70,** 1893 (1991).
5. G. Mak, Q. Fu, and H. M. van Driel, Appl. Phys. Lett. **60,** 542 (1992).
6. Q. Fu, G. Mak, and H. M. van Driel, Opt. Lett. **17,** 1006 (1992).
7. W. S. Pelouch, P. E. Powers, and C. L. Tang, Opt. Lett. **17,** 1070 (1992).
8. E. S. Wachman, W. S. Pelouch, and C. L. Tang, J. Appl. Phys. **70,** 1893 (1991).
9. W. S. Pelouch, P. E. Powers, and C. L. Tang, Opt. Lett. **17,** 1581 (1992).
10. E. C. Cheung and J. M. Liu, J. Opt. Soc. Am. B **8,** 1491 (1991).
11. D. A. Roberts, IEEE J. Quantum Electron. **28,** 2057 (1992).
12. Equations (2) and (3) are obtained by approximating $\delta_i^E \approx 0$ and $M_{j\mu} \approx 1$ in Eq. (28) in Ref. 11.
13. H. Vanherzeele and J. D. Bierlein, Opt. Lett. **17,** 982 (1992).
14. D. C. Edelstein, *New Sources and Techniques for Ultrafast Laser Spectroscopy,* Ph.D. dissertation (Cornell University, Ithaca, N.Y., 1990).
15. See, e.g., Y. R. Shen, *The Principles of Nonlinear Optics* (Wiley, New York, 1984), p. 79.
16. F. Ahmed, R. Belt, and G. Gashurov, Appl. Phys. Lett. **60,** 839 (1986).